Electronic Supplementary Material (ESI) for Soft Matter.

Supplementary Material for:

"Non-uniform Curvature and Anisotropic Deformation Control Wrinkling Patterns on Tori"

Xiaoxiao Zhang[1], Patrick T. Mather[2], Mark J. Bowick[3*], Teng Zhang[1†]

1. Department of Mechanical and Aerospace Engineering, Syracuse University, Syracuse, NY, 13244, USA

2. Department of Chemical Engineering, Bucknell University, Lewisburg, PA 17837 USA

3. Kavli Institute for Theoretical Physics, University of California, Santa Barbara, CA 93106, USA.

[*]bowick@kitp.ucsb.edu

[†]tzhang48@syr.edu

This file includes

1. Supplementary Methods

2. Supplementary figures and figure captions 1 to 3

1. Supplementary Methods

Finite element method for the wrinkles on tori

We performedd all simulations with the ABAQUS/standard solver. All the materials were described by a nearly incompressible neo-Hookean model, whose strain energy density can be expressed as

$$U = \frac{1}{2}\mu\left(J^{-\frac{2}{3}}I_1 - 3\right) + \frac{1}{2}\kappa(J-1)^2, \tag{1}$$

where μ is the shear modulus, κ is the Bulk modulus, I_1 represents the first invariant of the left Cauchy-Green deformation tensor, and J denotes the volumetric strain. To simplify the analysis, we chose the same Poisson ratio ($\nu = 0.475$) for all the materials by setting $\kappa/\mu = 20$.

The 3D structures were discretized using 20-node quadratic brick elements (C3D20R) with smallest mesh size 0.5, which is fine enough because we use high order elements. We modeled the isotropic expansion as thermal dilatation on the outer film to induce the compressive stresses and gradually increase the expansion to maintain a quasi-static process. This was achieved by decoupling the deformation tensor $\boldsymbol{F}$ into an elastic deformation part $\boldsymbol{A}$ and an expansion part $\boldsymbol{G}$.

$$\boldsymbol{F} = \boldsymbol{A} \cdot \boldsymbol{G}, \tag{2}$$

The isotropic expansion can be controlled by a scalar variable g

$$\boldsymbol{G} = \begin{bmatrix} 1+g & 0 & 0 \\ 0 & 1+g & 0 \\ 0 & 0 & 1+g \end{bmatrix}, \tag{3}$$

where $g > 0$. To trigger wrinkling instabilities, the positions of the surface nodes of the torus were randomly modified by a small increment relative to the mesh size.

2. Supplementary Figures, Figure Captions 1 to 3

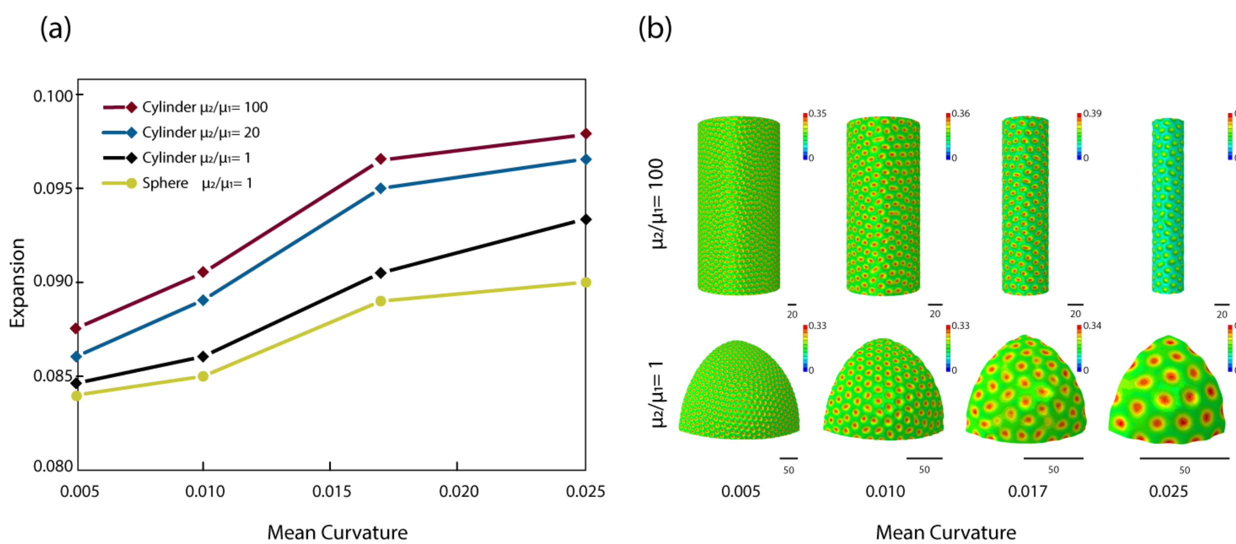

Fig. S1. Curvature delayed wrinkles in cylinders and spheres. (a) The critical expansion value of the onset wrinkle as a function of mean curvature. The inset figure shows the cross-section of the cylinders and spheres. To simplify the comparison, we keep $h = 1$ and a constant ratio between r_1 and r_2 (i.e., $r_1/r_2 =$

3) when changing the absolute value of the radius to vary the mean curvature. The mean curvature is calculated by h/r_1. (b) Simulation snapshots of the wrinkled configuration of cylinders and spheres at different mean curvatures. The colors indicate the maximum principal logarithmic strain. Note that we effectively simulate spherical bi-layer structures, as we already find the shear modulus of the inner core does not significantly influence the wrinkles in cylinders and spheres.

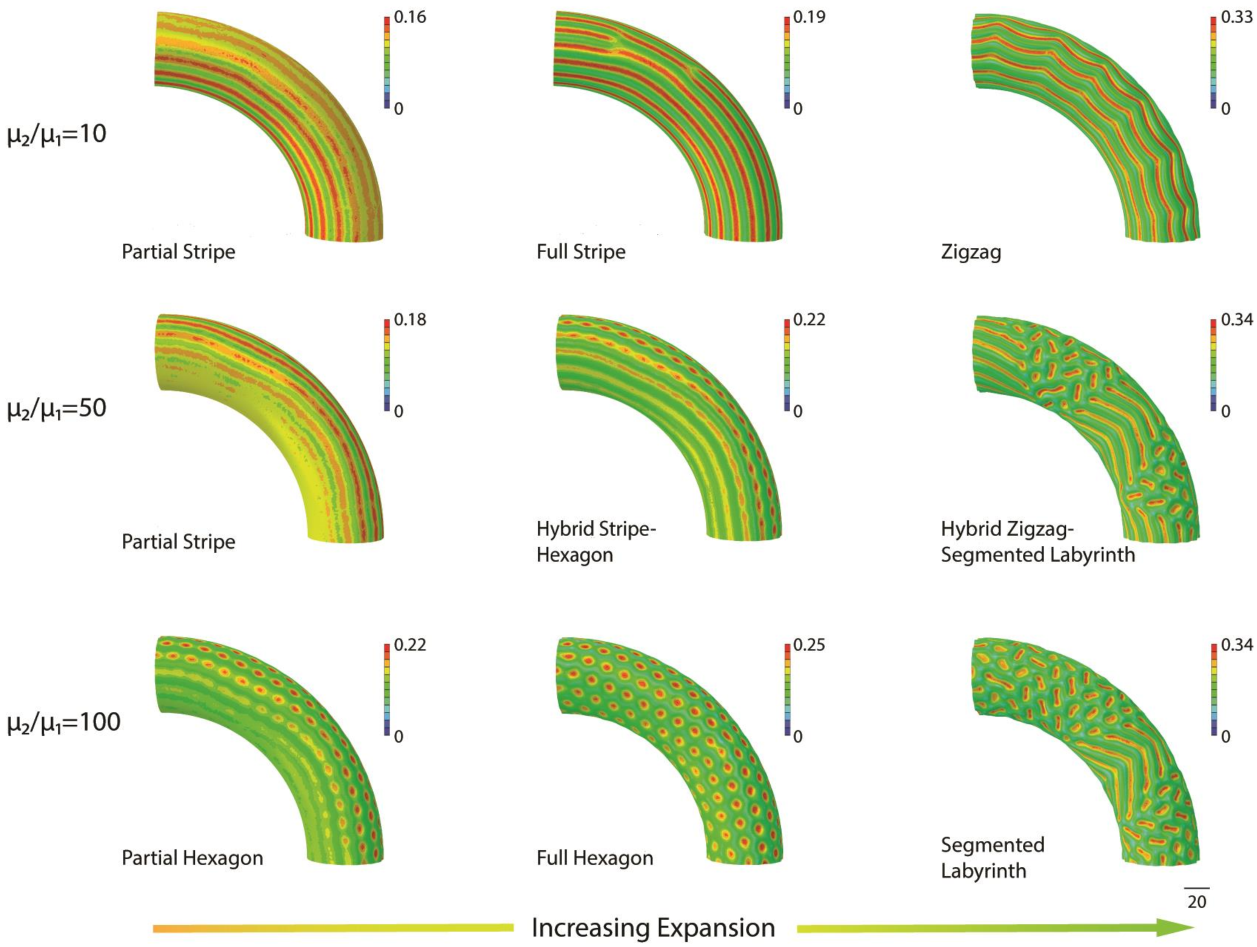

Fig. S2. Effect of the modulus ratio, between the outer film and the intermediate layer, on the formation and evolution of wrinkling patterns on a quarter of the torus. We set $\mu_0/\mu_1 = 20$ and keep all other material and geometric parameters the same as the simulations in Fig. 2.The different surface morphologies, from top to bottom, are displayed for varying elastic ratios $C = \mu_2/\mu_1$. The colors indicate the maximum principal logarithmic strain.

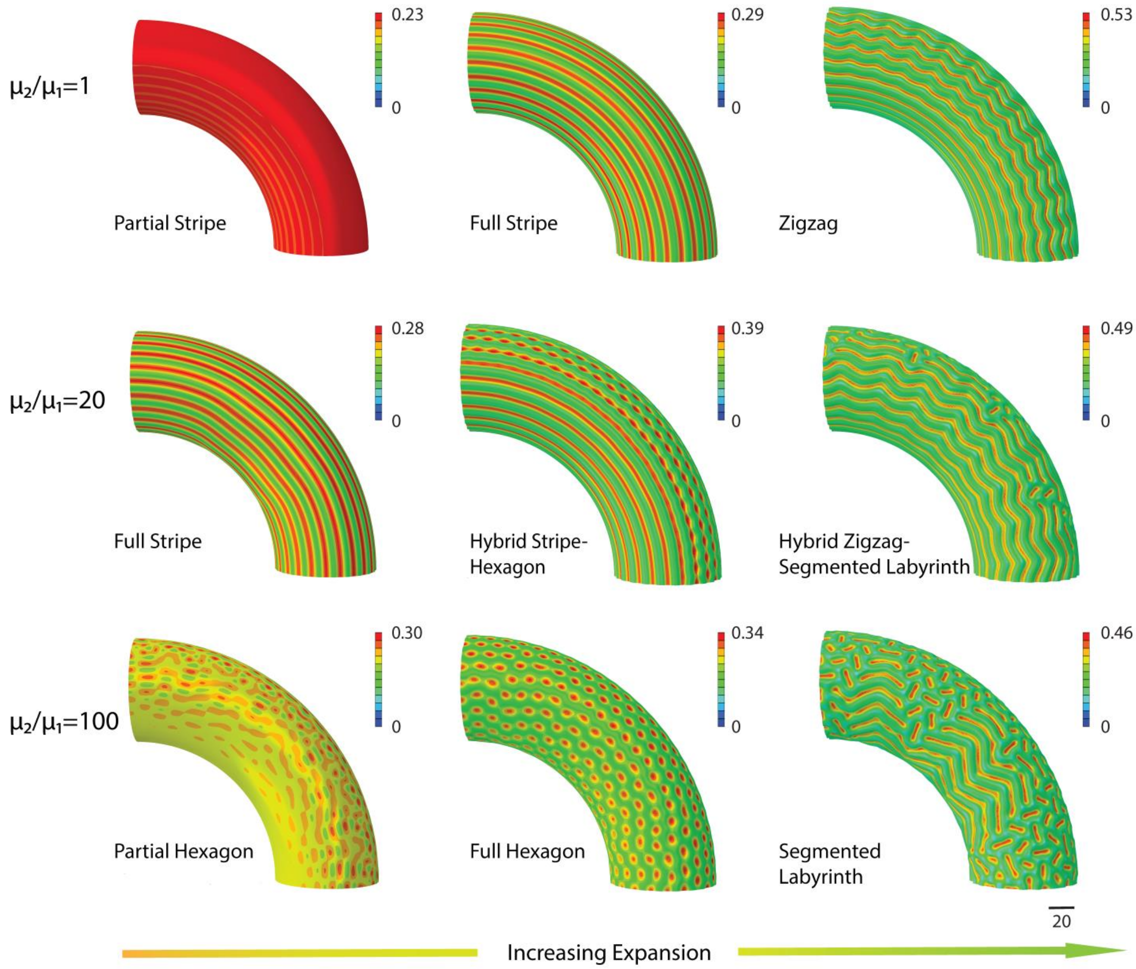

Fig. S3. Effect of the torus geometry on the formation and evolution of wrinkling patterns on a quarter of torus. We set $a = 41$ and keep all other material and geometric parameters the same as the simulations in Fig. 2.The different surface morphologies, from top to bottom, are displayed for varying elastic ratios $C = \mu_2/\mu_1$. The colors indicate the maximum principal logarithmic strain.